한국정밀공학회지 제 42 권 제 2 호 pp. 129-138 February 2025 / 129
J. Korean Soc. Precis. Eng., Vol. 42, No. 2, pp. 129-138 http://doi.org/10.7736/JKSPE.024.115
ISSN 1225-9071 (Print) / 2287-8769 (Online)

# 예비성형 금형설계를 통한 낙하산 하네스 부품의 단조공정에서 접힘 결함 개선

# Prevention of Folding Defects in the Forging Process of Parachute Harness Parts Through Preform Die Design

김정곤[1], 이성윤[1], 하진수[1], 한수빈[1], 권성욱[2], 고대철[3,#], 장진석[1,#]
Jeong Gon Kim[1], Sung Yun Lee[1], Jin Su Ha[1], Soo Bin Han[1], Seong Uk Kwon[2], Dae Cheol Ko[3,#], and Jin Seok Jang[1,#]

1 한국생산기술연구원 모빌리티부품그룹 (Advanced Mobility Components Group, Korea Institute of Industrial Technology)
2 ㈜대성단조 (Daesung Forge Co., Ltd.)
3 부산대학교 나노메카트로닉스공학과 (Department of Nanomechatronics Engineering, Pusan National University)
# Corresponding Authors / E-mail: jsjang@kitech.re.kr, TEL: +82-53-580-0152, ORCID: 0000-0002-6801-9109
E-mail: dcko@pusan.ac.kr, TEL: +82-51-510-3697, ORCID: 0000-0002-4064-739X

KEYWORDS: Pre-form die design (예비성형 금형 설계), Folding defects (접힘 결함), Forging process (단조 공정), Metal flow analysis (단류선 분석), Finite element analysis (유한요소해석)

*This study focuses on preventing folding defects in the forging process of parachute harness parts. Through three-dimensional finite element analysis, it was determined that folding defects arise from uneven metal flow and timing differences in the filling of various regions. To address these issues, a preform die was designed and evaluated using multi-stage forging simulations. The results indicated that the preform die facilitated uniform metal flow, preventing folding defects and ensuring consistent filling across all key areas. To verify the simulation results, surface and cross-sectional metal flow analyses were conducted. Additionally, the preform die reduced the maximum die load, which is expected to extend die lifespan and improve overall process efficiency. These findings demonstrate that precise control of metal flow and the application of a preform die can significantly enhance the quality and durability of forged components, providing valuable insights for improving forging processes across various industries.*

Manuscript received: September 19, 2024 / Revised: November 1, 2024 / Accepted: November 25, 2024

## 1. Introduction

Hot forging is a process that shapes heated material by plastically deforming it using a die. After forming, the material conforms to the die's shape, resulting in superior structural strength due to improved metal flow compared to other methods [1]. This enhanced strength makes hot forging suitable for components requiring high reliability under extreme conditions, such as aerospace applications [2,3].

Parachute harness parts in the aerospace field are produced by forging to ensure their durability and reliability. When a parachute deploys and descends, various loads including tension, impact, and compression forces occur simultaneously and can be quite substantial. As these harness parts play a critical role in supporting the stable deployment and descent of the parachute, it is essential to utilize a high-quality forging process to maintain structural strength under these diverse load conditions [4,5].

Defects that degrade quality in the forging process include folding defects, which cause stress concentrations in the parts and reduce strength and fatigue life [6]. The causes of folding defects can occur during the metal flow merging from multiple directions, when the flow speed of the metal varies across different areas of the die cavity, or due

to deterioration in the surface quality of the initial billet [7].

To address these folding defects, solutions can be implemented such as designing a preform die, making localized modifications to existing dies, or adjusting process parameters [8,9]. However, the selection and implementation of these methods depend on the designer's experience and trial and error, which can be costly and inefficient. Folding defects primarily occur in plastic deformation processes like forging, which are performed under large loads and complex stress states, and where significant variations in strain and stress distribution occur. Because of this, research using finite element analysis (FEA) is actively conducted to identify the causes of defects and develop solutions [10,11]. Finite element analysis can accurately predict folding defects and metal flow during the forging process [12].

Analysis through metal flow prediction is typically conducted using two-dimensional symmetric analysis under plane strain and axisymmetric conditions [13,14]. While two-dimensional metal flow lines allow for the observation and analysis of metal flow in the cross-sections of cut products, the complex shapes of harness parts and their dies with irregular flows necessitate three-dimensional metal flow line analysis. Three-dimensional flow lines can be generated and predicted on the surfaces and cross-sections of metal materials. Surface metal flow lines help identify folding defects through irregularities or breaks in the lines, and flow lines on cross-sections can reveal the depth of internal folding defects.

In this study, DEFORM-3D, an FEA software, was utilized to analyze folding defect causes and explore solutions [12]. Forming analysis was conducted on circular initial billet and forging dies to observe metal flow during the process, and flow patterns were examined to assess folding defects. Based on simulation results, a preform die was designed to minimize defect formation, and multi-stage forging analysis was performed to verify its effectiveness. Design validity was evaluated through simulation outcomes, followed by prototype production, and observed metal flow patterns in the specimen were compared with simulation predictions to confirm design adequacy.

## 2. Current Forging Process of Harness Parts

The current forging process for harness parts includes 1st forging, trimming, annealing, and 2nd and 3rd forging stages, as shown in Fig. 1. These three-stage forging dies were manufactured with cavities identical in dimensions and shape to the final product.

The 1st forging is carried out through hot forging, with a gap of 1.5 mm set between the upper and lower dies. This gap ensures proper volume distribution of the material to prevent defects such as folding, underfill, and overloading in subsequent processes. Material pushed outside the die cavity during forming is called flash, which is removed during the trimming process. Annealing is conducted to remove internal stresses caused by hot forging and trimming, enhancing forgeability. 2nd forging is also carried out through hot forging, shaping to the final dimensions with a die gap of 1.2 mm. This gap compensates for the metal shrinkage and oxide scale that occur after hot forging, which can reduce surface quality and dimensional accuracy. The final step, 3rd forging, is the sizing stage completed at room temperature to finalize the shape, correcting any shrinkage and surface defects from the previous hot forging, thus ensuring the final product quality.

Gutter designs have been applied to the 2nd and 3rd forging dies to minimize the excessive load caused by flash, as illustrated in Fig. 2. Figs. 2(a) shows the 1st forging die, while 2(b) represents

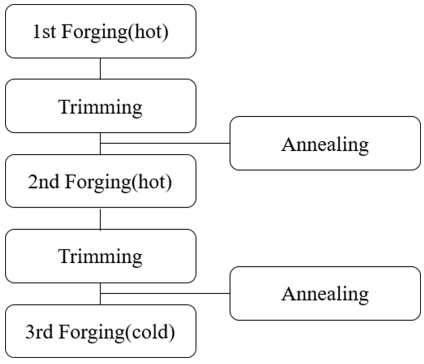


Fig. 1 The current forging process for harness parts

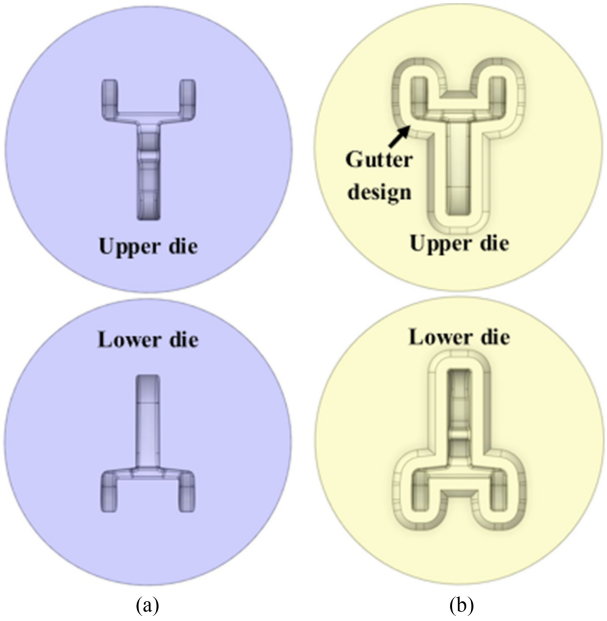


Fig. 2 Forging die design: (a) 1st forging die and (b) 2nd and 3rd forging die

the 2nd and 3rd forging dies. The hot forging die material is QHZ, a high-speed tool steel that maintains hardness and heat resistance even at high temperatures, allowing for forging. The cold forging die material is QCM8, which requires high strength and toughness in cold forging, offering better wear resistance and toughness than the carbon tool steel SKD11. The equipment used is a crank-type mechanical press with a permissible load of 1,000 tons. The material is SCM440, an alloy steel containing chromium and molybdenum.

## 3. Analysis of the Current Forging Process

### 3.1 Defect Analysis in 1st Forging

In 1st forging, basic shaping is performed to properly distribute the volume and prevent defects that may occur during final forming. To review the process, a single forging was conducted at 70% of the forming conditions with the 1st forging die and initial billet, and the results are shown in Fig. 3. Harness parts are categorized into hook, neck, and snap sections. Upon inspecting the 1st forged product, folding defects were identified in the snap, which led to the defects being magnified and analyzed through image processing. The folding defects occurred at two points in the snap: Folding A occurred horizontally at the boundary between the filled and unfilled areas, while Folding B occurred vertically in the unfilled area.

Fig. 3 illustrates that defects occurred even before the forming process was complete, highlighting the need for a comprehensive analysis of the entire process, including the final stage. To determine the causes of these folding defects and propose solutions, FEA was conducted using DEFORM-3D.

### 3.2 Conditions for the 1st Forging FEA

A three-dimensional analysis was conducted to examine the characteristics of volumetric forming and the irregular metal flow occurring during the forging process. Fig. 4 illustrates the position of the 1st forging die and the initial billet. The material, produced through extrusion, is cylindrical, with a diameter of 25 mm and a length of 120 mm. Choi demonstrated that temperature minimally affects metal flow prediction in forging processes. This study applied isothermal analysis to minimize temperature variation effects on metal flow [15]. The parameters used in the analysis reflect actual process data and are summarized in Table 1. Maximum stroke denotes the equipment's maximum allowable stroke, while forging stroke specifies the amount of deformation applied during the 1st forging process. The friction model utilized shear friction, effectively representing the high temperatures and plastic deformations of forging process [16].

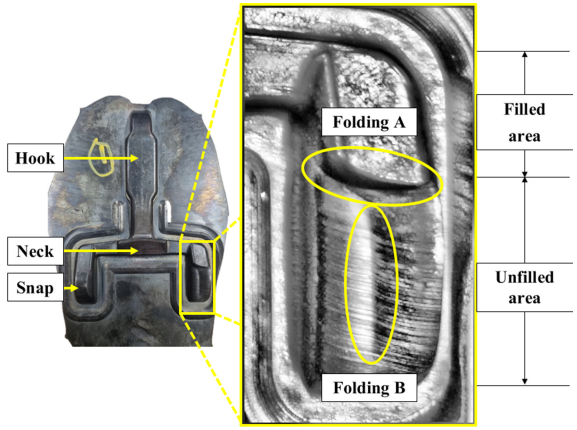


Fig. 3 Prototype produced by 1st forging

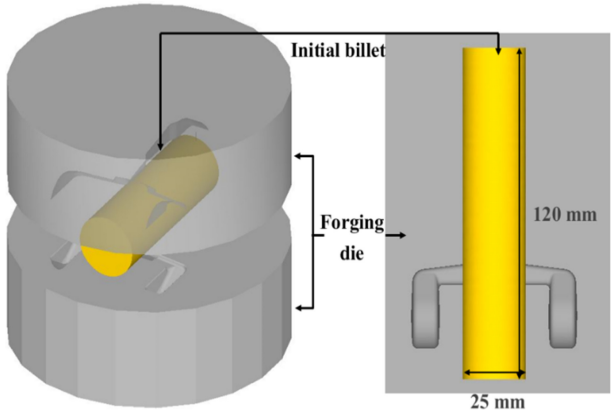


Fig. 4 Die and initial billet position for 1st forging

Table 1 Parameters of simulation

| Parameters | Value |
|---|---|
| Friction factor | 0.3 |
| Maximum stroke | 220 mm |
| Forging stroke | 23.5 mm |
| Average punch velocity | 318 mm/sec |
| Number of mesh elements for billet | 110,000 |
| Die temperature | 400 ºC |
| Initial billet temperature | 900 ºC |

### 3.3 Results of Analysis

The cavity in the center of the die begins to fill first due to the position of the die and the initial billet. Then, the material moves towards the snap through the compression of the die, completing the filling and forming process. The results of the 1st forging analysis are shown in Fig. 5. Fig. 5(a) shows the stage of forming where folding defects were found, with Folding A and B being identical to those in the initial product, and their positions and shapes matching. To view the surface metal flow prediction, surface metal flow lines were generated on the initial billet, as

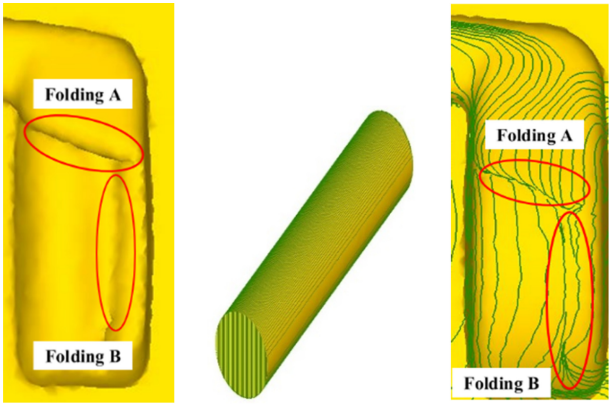


(a) (b) (c)

Fig. 5 1st forging simulation results: (a) Folding defects during forming, (b) Surface metal flow of the initial billet, and (c) Folding defects predicted by surface metal flow analysis

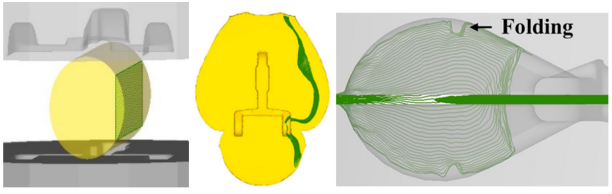


(a) (b) (c)

Fig. 6 Cross-sectional metal flow prediction results: (a) Cross-sectional metal flow of initial billet, (b) Simulation results, and (c) Cross-sectional metal flow of folding defect

shown in Fig. 5(b). Fig. 5(c) shows the predicted metal flow at the completion of the 1st forging. Folding defects were also confirmed through the metal flow prediction at the point of completed forming. The surface length of Folding A is approximately 7 mm, and Folding B is approximately 12 mm.

To confirm the internal metal flow and folding depth of the snap where folding defects occurred, the cross-sectional metal flows were predicted and analyzed. The results are shown in Fig. 6. As shown in Fig. 6(a), metal flows were generated on the cross-section of the right side of the initial billet, and the predicted cross-sectional metal flows at the completion of the forging process are shown in Fig. 6(b). Fig. 6(c) provides a side view of the snap where surface folding defects were observed in Fig. 5, and internal folding defects were confirmed through the cross-sectional metal flows. The internal metal flow of the 1st forged part was examined, and a folding depth of 2 mm was found.

Fig. 7 shows the stress concentration occurring in the folding area as the folding defect progressed, with a maximum effective stress of 454 MPa. This stress concentration renders the part susceptible to fatigue failure and can reduce the lifespan of the component under repeated loading conditions.

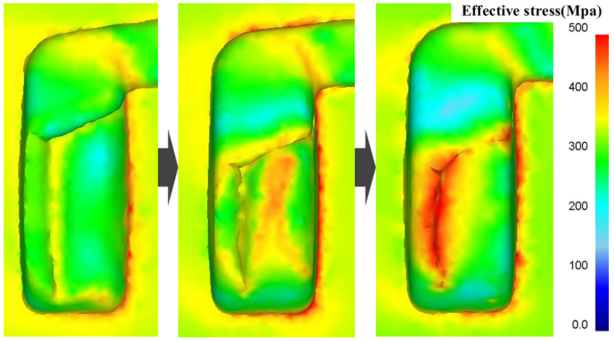


Fig. 7 Effective stress concentration due to folding defect progression

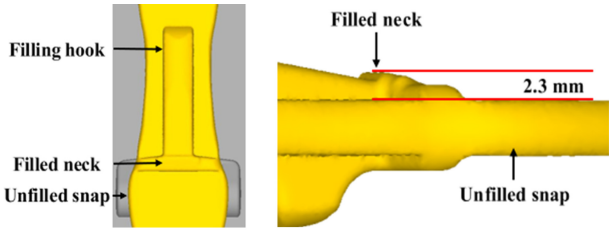


(a) (b)

Fig. 8 Formed to a state of 17 mm: (a) Top view and (b) Side view

### 3.4 Causes of Folding Defects

To determine the primary cause of folding defects observed in the 1st forging simulation, the forming process was analyzed in detail. Fig. 8 shows the material state after compressing 17 mm out of a total 23.8 mm press stroke. Figs. 8(a) presents a top view, while 8(b) shows a side view for clearer understanding. At this stage, the hook, with a larger die cavity volume, is still filling, whereas the neck, with a smaller cavity volume, has already filled completely. In Fig. 8(a), the snap section has not begun filling, as there is still a gap between the snap and the initial billet. Additionally, Fig. 8(b) shows a 2.3 mm difference in level between the neck and the snap, resulting from their differing filling states.

To understand how the differences in filling progress and resulting level differences contribute to folding defect formation, Fig. 9 illustrates the forming process from the appearance of the level difference to the identification of the folding defect. Fig. 9(a) shows the state after 17 mm of forming, with the neck section fully filled. As the press continues, the flash moves toward the snap section. Fig. 9(b) illustrates the state after 19 mm of forming, where the flash is pushed into the snap cavity by the compressive force of the press. In Figs. 9(a), the flash displays only lateral flow, but in 9(b), the snap cavity offers more space, resulting in additional longitudinal flow. Fig. 9(c) shows the state after 20 mm of forming, where the snap section begins to fill, driven by both the flash and the metal flow from the already filled neck section. At this stage, a boundary

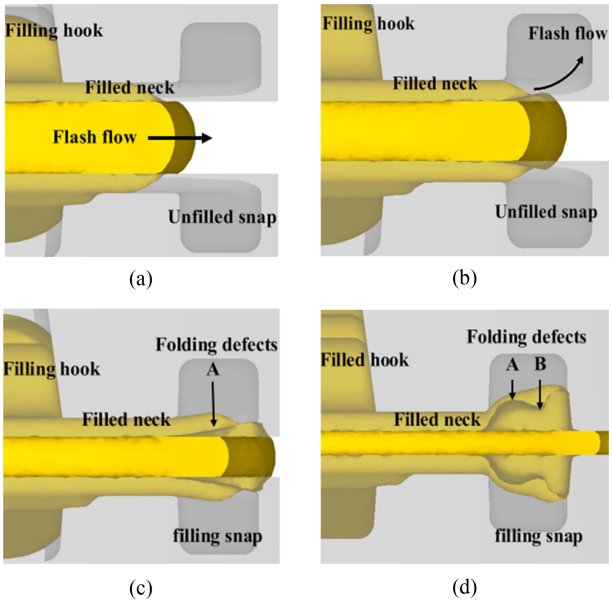


Fig. 9 Front view until detection of snap folding defect: (a) Forming stroke 17 mm, (b) Forming stroke 19 mm, (c) Forming stroke 20 mm, and (d) Forming stroke 22 mm

between filled and unfilled areas appears in the snap section, leading to the formation of Folding A. Fig. 9(d) depicts the state after 22 mm of forming, where the snap section fills from two different areas. The flash filling observed in Figs. 9(b) and 9(c), driven by both lateral and longitudinal metal flow, results in the filling shown in 9(d). This difference in filling degree between the inner and outer regions of the snap section leads to the formation of Folding B. Forming process analysis confirmed that the primary cause of folding defects is the difference in forming progress between the neck and snap sections.

## 4. Design and Verification of the Preform Die

### 4.1 Preform Die Design

To address the two long, deep folding defects identified in the existing 1st forging die, a preform die was designed to improve timing differences across sections, replacing the existing 1st forging process. The improved forging process, shown in Fig. 10, meets the objectives of the existing 1st forging while preventing folding defects. Additionally, the existing 2nd and 3rd forging processes were reordered as the 1st and 2nd forging stages, respectively. This adjustment retains the total number of processes while enhancing overall quality and performance.

The preform die must meet the following conditions: First, the ratio of material diameter to length must not exceed 2.3 to prevent buckling during preforming [17]. Exceeding this ratio can cause buckling during forming, compromising structural stability. To prevent

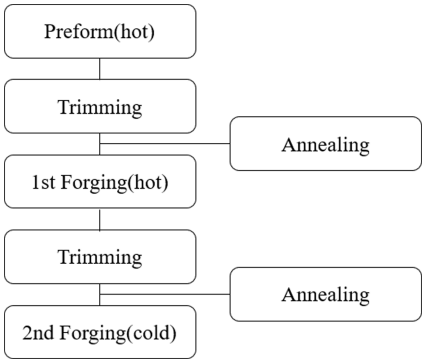


Fig. 10 Improved forging process for harness parts

buckling, it is essential that the initial billet required to form the hook remains undeformed. Second, the preform die must meet preforming requirements for the snap section. Third, the preformed part must be free of folding defects to ensure the final product's quality. The preform die design must be precise to satisfy these conditions.

The preform die was designed by analyzing the characteristics of the upsetting and heading processes. In the conventional process, the material is compressed lying flat, but in the preforming process, it is compressed upright, enabling the upper die to preform the snap while the material in the lower die retains its original shape. Typically, in the upsetting process, an unshaped upper die compresses the initial billet, causing expansion in the radial direction. However, since the snap's center is hollow, the material expands bilaterally as the upper die compresses, with the die designed to leave the center unfilled. This design enables the material needed for the snap to expand, completing its preformed shape. The upper and lower dies were designed with a diameter-to-length ratio of 2.2 to ensure stability against buckling.

Fig. 11 shows the cross-sections of two types of improved preform dies. Figs. 11(a) and 11(b) represent the cross-sections of Case 1, while 11(c) and 11(d) represent those of Case 2. The Case 1 die was designed to closely approximate the final product dimensions, but due to the nature of semi-closed forging, it does not achieve complete filling at the end of the forming process. This design considers the limitations of the forging equipment, which does not allow for automatic ejection, and any insufficient forming can be compensated through additional forging in the subsequent process. In contrast, the Case 2 die was designed with less deformation compared to Case 1, following the characteristics of a typical closed-die forging process, and was intended to achieve complete filling at the end of forming. A 1-degree expansion angle was added to the center of the lower die cavity for easier product removal. The key dimensions are presented in Table 2. Multi-stage forging simulations, including preforming and 2nd forging for both Cases 1 and 2 dies, were conducted, and the results were compared to select the preform die that produced the best outcome.

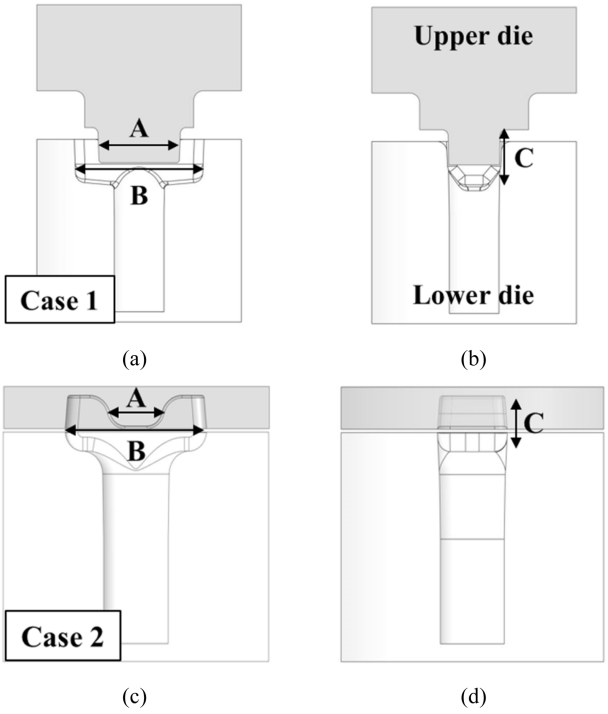


Fig. 11 Shape of the preform die: (a) Front view of Case 1, (b) Side view of Case 1, (c) Front view of Case 2, and (d) Side view of Case 2

Table 2 Comparison of key dimensions between Cases

| Design parameters | Final product | Case 1 | Case 2 |
|---|---|---|---|
| A [mm] | 43.2 | 41 | 20.4 |
| B [mm] | 64.3 | 65.5 | 56 |
| C [mm] | 28.5 | 28 | 18.4 |

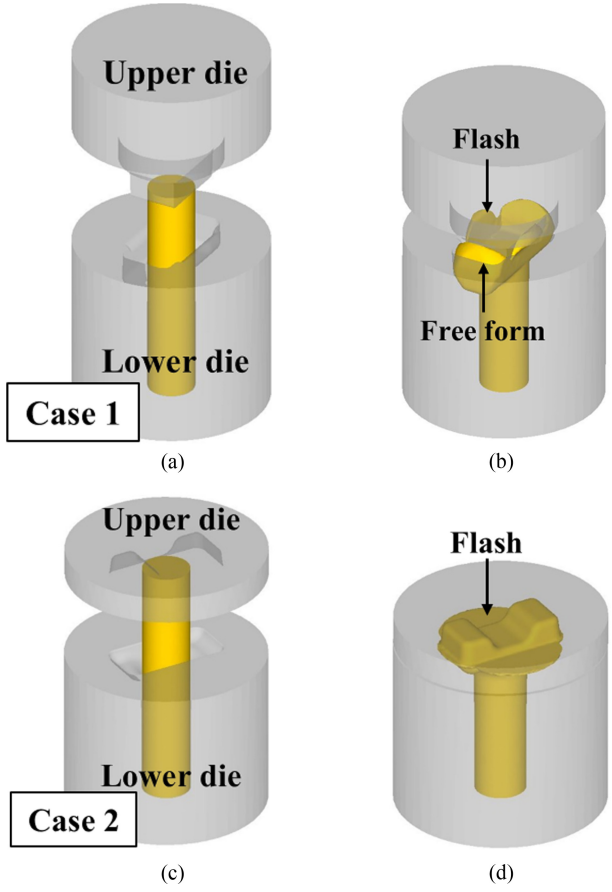


Fig. 12 Preform results: (a) Before preform of Case 1, (b) After preform of Case 1, (c) Before preform of Case 2, and (d) After preform of Case 2

### 4.2 Conditions of Multi-stage Forging Analysis

To assess the effectiveness of the preform dies, a multi-stage forging analysis was conducted. Multi-stage forging analysis evaluates the forging process by forming a product through multiple dies using a single material. The analysis followed the sequence of preforming, trimming, and 1st forging stages. The preform die strokes were set to 41 mm for Case 1 and 45 mm for Case 2, reflecting structural differences. The 1st forging stroke was set at 23.8 mm. Apart from the forming stroke, parameters like the friction coefficient, maximum stroke, and stroke speed matched the conditions in Table 1.

### 4.3 Results of Analysis

Fig. 12 presents the forming results of the initial billet with the designed preform dies. Figs. 12(a) and 12(b) depict the before and after states for Case 1, while 12(c) and 12(d) show the corresponding states for Case 2. The initial billet was compressed by the upper die, reflecting characteristics of the upsetting and heading processes, which increased its diameter. The expanded billet then moved into the snap cavity of the preform lower die, completing filling and forming. Any unformed flash was extruded outside the die cavity. Due to differences between the Cases 1 and 2 dies, the shape of the extruded flash varied. The Case 1 die exhibited semi-closed forging characteristics, maintaining critical snap dimensions while leaving other areas uncontrolled by the die cavity. In contrast, the Case 2 die followed the closed-die forging method, filling all areas within the die cavity and fully controlling metal flow.

The analysis of the 1st forging process was performed following preforming and trimming, and the results for both cases are shown in Fig. 13. Figs. 13(a) and 13(b) display the results before and after the 1st forging process for Case 1, whereas 13(c) and 13(d) present the corresponding results for Case 2. was performed after aligning the preformed part with the die cavity. The gutter design of the forging die resulted in folding and flash formation at the snap and neck shear areas, as shown in Figs. 13(b) and 13(d). The flash shape varied owing to differences in the preform die specifications.

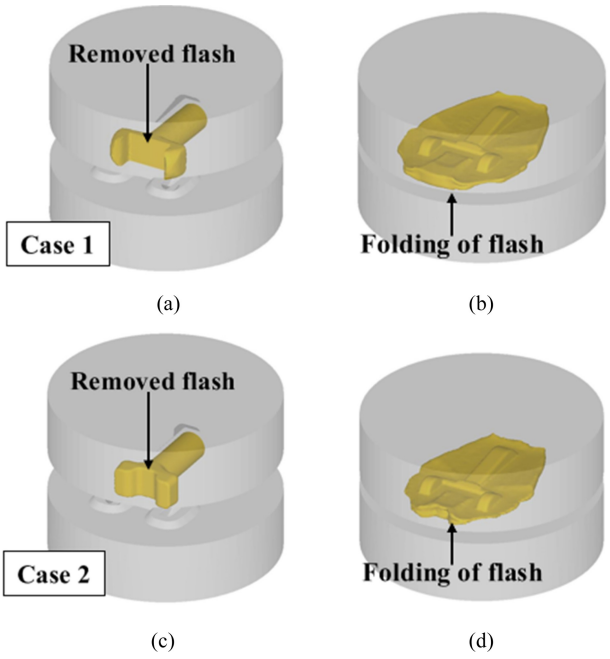


Fig. 13 1st forging results: (a) Before 1st forging of Case 1, (b) After 1st forging of Case 1, (c) Before 1st forging of Case 2, and (d) After 1st forging of Case 2

This flash will be removed by trimming before the cold forging stage.

To confirm simultaneous formation of all areas hook, neck, and snap as required by the preform die design, the forming state at a 17 mm stroke, where a material step was observed in Fig. 8, was compared and displayed in Fig. 14. Figs. 14(a) presents the forming result for Case 1, and 14(b) shows that for Case 2. Both preform die designs indicate that filling began simultaneously across all areas. However, while snap filling was completed in Case 1, it remained in progress in Case 2.

Finally, die load for the two preform die cases was compared. Die load has a significant effect on die lifespan and the quality of the forged product. Excessive load can reduce die lifespan, necessitating more frequent replacements and negatively affecting productivity. Fig. 15 displays the load results for the two cases. The maximum load measured in Case 1 was 94 tons, while in Case 2, it reached 283 tons. Die load in Case 1 was about one-third lower, as the Case 1 die had semi-closed characteristics, preventing complete filling of the die cavity. Conversely, the Case 2 die was a closed die, designed to ensure full cavity filling by the billet. Additionally, the Case 1 die was designed to minimize extra contact and resistance from the flash, avoiding major increases in die load. In contrast, in Case 2, the upper die continued compressing the flash after expulsion, causing additional deformation. This increased the contact area between the die and material, leading to higher resistance and a rise in die load.

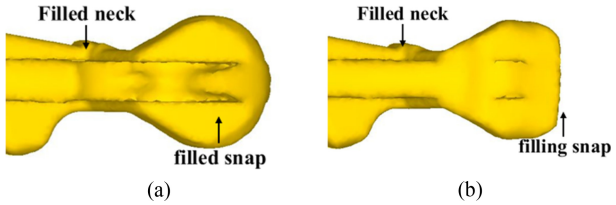


Fig. 14 Comparison of forming states at a 17 mm stroke for both preform die designs: (a) Case 1, and (b) Case 2

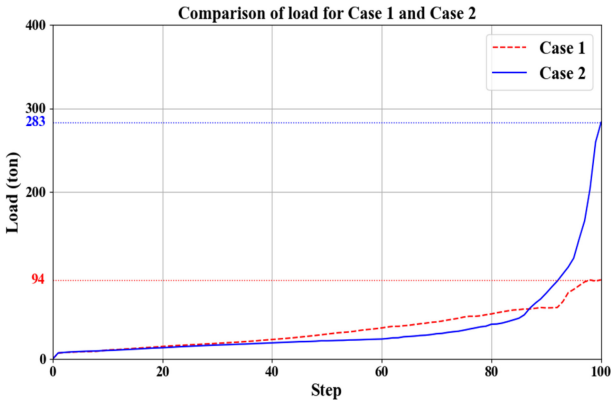


Fig. 15 Comparison of die load for Case 1 and Case 2

As a result of comparing the two dies, the Case 1 die was selected as the preform die due to its advantages of achieving a shape closer to the final form, promoting smoother metal flow, and exhibiting lower die load, which can improve die lifespan and productivity.

An analysis of the effective stress flow in the folding sections was conducted to quantitatively compare the selected die with an existing die. However, because the preform die and the existing 1st forging die differ structurally, a direct comparison of the effective stress flow may not be reliable. To address this, we utilized the process characteristic in which the cavity shapes and dimensions of the existing 1st and 2nd forging dies are identical. The formed state of the existing 1st forging die is dimensionally and geometrically identical to the state achieved after the preforming and 1st forging, allowing for a reliable comparison of the maximum effective stress in the effective stress flow. The comparison results are shown in Fig. 16. The maximum value of the effective stress flow after the improvement was reduced to 312 MPa, which represents a decrease of approximately 31.3%.

## 5. Metal Flow Analysis in the Improved Forging Process

To observe the presence of folding defects in the formed parts with the preform die, multi-stage forging process analysis and three-dimensional metal flow predictions were conducted, and the

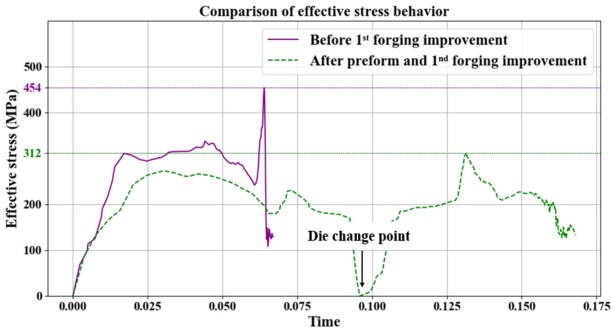


Fig. 16 Comparison of effective stress behavior

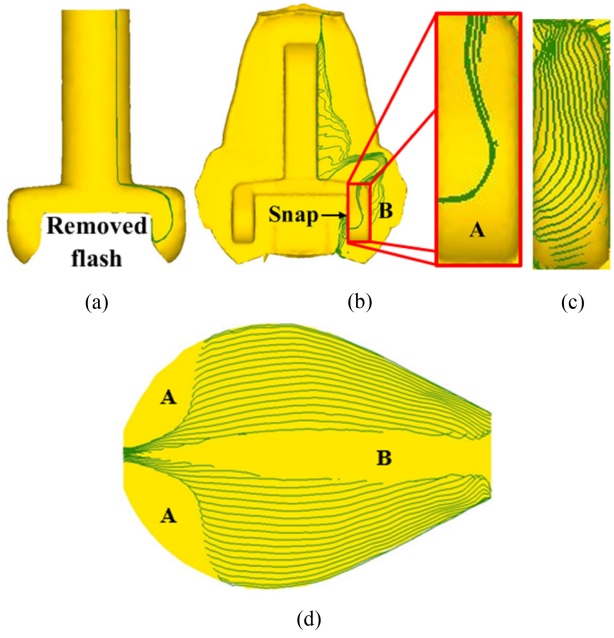


Fig. 17 Predicted metal flow and folding defect FEA in multi-stage forging: (a) Cross-sectional metal flow lines in the preform stage after trimming, (b) Metal flow lines in the 1st forging stage, (c) Predicted surface metal flow lines, and (d) 3D cross-sectional metal flow lines in the snap section

results are shown in Fig. 17. Fig. 17(a) illustrates the predicted cross-sectional metal flow lines on the snap after trimming to remove the flash following the preforming. Fig. 17(b) presents the forming and metal flow predictions up to the 1st forging step. Most of the metal flow lines generated during the preforming moved into the flash region. Figs. 17(c) shows the predicted surface metal flow lines, where the folding defects observed in 5(c) were reduced, indicating a smoother metal flow, consistent with the cross-sectional metal flow in Fig. 17(b). Fig. 17(d) shows the three-dimensional cross-sectional metal flow within the snap, including the metal flow information in the thickness direction. The two sections without identifiable metal flow lines are shown in Fig. 17(d). Section A corresponds to the shear section of the snap,


Fig. 18 Specimen production in multi-stage process: (a) After preform, (b) After forging, and (c) After trimming

where, as shown in the enlarged view in Fig. 17(b), the cross-sectional metal flow lines do not extend to the shear section, but instead move into the flash region, resulting in no visible metal flow lines in Section A. Section B corresponds to the metal flow lines formed within the flash during the forming process, which were removed to improve the visibility of the metal flow within the snap. Cross-sectional metal flow predictions confirmed a smooth metal flow with the application of the preform die, and no folding defects were observed.

Fig. 18 shows the prototype manufacturing process of the multi-stage process using the preform die and the 1st forging die. Fig. 18(a) shows the preformed part after the 1st process. The preform die satisfied the design criteria, and buckling did not occur during the forming process. In addition, the preformed shape of the snap matched the analysis results. Fig. 18(b) shows the forged part formed using the 1st forging die on the preformed part. Fig. 18(c) shows the prototype after trimming the forged part. Through preforming, simultaneous forming of all areas in the 1st forging process was achieved, and no folding defects were observed on the surface of the prototype, confirming that the preform die met the intended design criteria.

To verify the results of the metal flow analysis, a metal flow experiment was conducted using a prototype specimen. First, the snap of the specimen was cut vertically through the center to obtain a cross-sectional sample of the snap. Contaminants on the surface of the cut section were removed during the cutting process. The etchant was prepared using distilled water and hydrochloric acid at a 1:1 ratio. The temperature of the etchant was maintained at 80 ºC and the specimen was immersed for 30 min for etching. After etching, the specimen was rinsed with distilled water and dried to observe the cross-sectional surface. A comparison of the metal flow experiment and the analysis results is shown in Fig. 19. The results indicated a metal flow similar to the predicted metal flow, with no folding defects. This provides important evidence supporting the validity of die design and demonstrates that analysis-based predictions are reliable in actual processes.

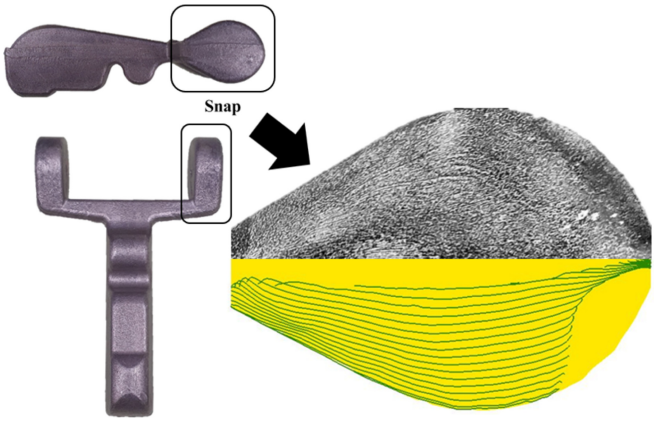


Fig. 19 Comparison of metal flow experiment and prediction results

## 6. Conclusion

This study presented various approaches to prevent folding defects that occur in the forging process. The research results can be summarized as follows:

(1) Through three-dimensional finite element analysis, it was confirmed that folding defects arise from differences in material levels and the resulting uneven filling times. This highlights the necessity for precise analysis of metal flow to address folding defects in the forging process.

(2) A preform die was designed to prevent folding defects. Multi-stage forging analysis using the preform die confirmed that filling occurred simultaneously in all areas of the die, demonstrating that the preform die effectively prevents folding defects.

(3) After applying the preform die, the surface folding defects of 12 and 7 mm and a depth of 2 mm in the snap area were improved, and the resulting effective stress was reduced by approximately 31.3%. The final product demonstrated superior structural strength and durability compared to the conventional process.

(4) The metal flow experiment confirmed that the folding defects were improved and that the metal flow path was consistent with the simulation results. This proves that the simulation results are reliable in actual product manufacturing.

This study emphasizes the necessity of preform die design to address folding defects, demonstrating that stable and high-strength products can be manufactured. These findings are expected to contribute to quality improvements in forging processes across various industries, including aerospace components.

## ACKNOWLEDGEMENT

This work was partly supported by the Convergence Production Advancement Technology Development Project of the Korea Institute of Industrial Technology [No. KITECH-EH-25-0003] and the Development of New Products Subject to Purchase Conditions of MSS [No. S3345198].

## REFERENCES

1. Eom, J. G., Jeong, S. W., Joun, M. S., (2013), Metal forming simulation with emphasis on metal flow lines and its applications, Transactions of Materials Processing, 22(6), 233-327.
2. Gronostajski, Z., Pater, Z., Madej, L., Gontarz, A., Lisiecki, L., Lukaszek-Solek, A., Luksza, J., Mroz, S., Muskalski, Z., Muzykiwicz, W., Pietrzyk, M., Sliwa, R. E., Tomczak, J., Wiewiorowska, S., Winiarski, G., Zasadzinski, J., Ziolkiewicz, S., (2019), Recent development trends in metal forming, Archives of Civil and Mechanical Engineering, 19, 898-941.
3. Behrens, B.-A., Volk, W., Maier, D., Scandola, L., Ott, M., Brunotte, K., Buedenbender, C., Till, M., (2020), A combined numerical and experimental investigation on deterministic deviations in hot forging processes, Procedia Manufacturing, 47, 295-300.
4. Grim, R., Popela, R., Jebáček, I., Horák, M., Šplíchal, J., (2023), Determination of the parachute harness critical load based on load distribution into individual straps with respect of the skydiver's body position, Aerospace, 10(1), 83.
5. Zhang, S. Y., Yu, L., Masarati, P., Qiu, B. W., (2022), New general correlations for opening shock factor of ram-air parachute airdrop system, Aerospace Science and Technology, 129, 107844.
6. Gao, P., Yan, X., Fei, M., Zhan, M., Li, Y., (2019), Formation mechanisms and rules of typical types of folding defects during die forging, The International Journal of Advanced Manufacturing Technology, 104, 1603-1612.
7. Ge, X., Yu, Y., Yu, H., Wang, G., (2023), Study on folding defect elimination method of track link forging based on preforming design, International Journal of Precision Engineering and Manufacturing, 24(1), 61-71.
8. Chiang, M.-Y., Hu, J.-W., Hsiao, T.-C., Tsai, M.-C., Huang, S.-C., (2023), The optimization design of pre-forming for forging automobile parts using taguchi method based grey relational analysis, Advances in Mechanical Engineering, 15(6), 16878132231183531.
9. Seo, W., Min, B., Park, K., Ra, S., Lee, S., Kim, J., Kim, J., (2011), Design of cold heading process of a screw for storage parts, Transactions of Materials Processing, 20(1), 48-53.

10. Ko, D. C., An, J. H., Jang, M. J., Bae, J. H., Kim, C. H., Kim, B. M., (2008), Process design of seat rail in automobile by the advanced high strength steel of dp780, Transactions of Materials Processing, 17(3), 197-202.

11. Song, W.-J., Heo, S.-C., Ku, T.-W., Kim, J., Kang, B.-S., (2008), Evaluation of formability on hydroformed part for automobile based on finite element analysis, Transactions of Materials Processing, 17(1), 52-58.

12. Obiko, J. O., Mwema, F. M., Bodunrin, M. O., (2019), Finite element simulation of X20CrMoV121 steel billet forging process using the Deform 3D software, SN Applied Sciences, 1, 1044.

13. Ku, T. W., (2023), Residual stress prediction and hardness evaluation within cross ball grooved inner race by cold upsetting process, Transactions of Materials Processing, 32(4), 180-188.

14. Razali, M. K., Kim, S. W., Irani, M., Kim, M. C., Joun, M. S., (2021), Practical quantification of the effects of flow stress, friction, microstructural properties, and the tribological environment on macro- and micro-structure formation during hot forging, Tribology International, 164, 107226.

15. Choi, M. H., Jin, H. T., Joun, M. S., (2015), Effect of flow stress, friction, temperature, and velocity on finite element predictions of metal flow lines in forgings, Transactions of Materials Processing, 24(4), 227-233.

16. Matsumoto, R., Osumi, Y., Utsunomiya, H., (2014), Reduction of friction of steel covered with oxide scale in hot forging, Journal of Materials Processing Technology, 214, 651-659

17. Jhonthong, N., Talangkun, S., (2023), Design of the semi-closed die for shaping the thick coin-like carbon steel parts in a single operation, SN Applied Sciences, 5, 176.

**Jeong Gon Kim**
is currently an M.S. candidate in the Department of Nanomechatronics Engineering at Pusan National University, Busan, Korea, and is a member of the Advanced Mobility Components Group at the Korea Institute of Industrial Technology (KITECH). His research interests include plastic deformation and forging processes.
E-mail: r4r5t@kitech.re.kr

**Sung Yun Lee**
is a senior researcher at the Advanced Mobility Components Group of the Korea Institute of Industrial Technology (KITECH). His research interests include materials science and plastic deformation processes.
E-mail: yunskills@kitech.re.kr

**Jin Su Ha**
is currently a Ph.D. candidate in the Department of Nanomechatronics Engineering at Pusan National University, Busan, Korea, and is a member of the Advanced Mobility Components Group at the Korea Institute of Industrial Technology (KITECH). His research interests include materials science and deep learning.
E-mail: jinsu302@kitech.re.kr

**Soo Bin Han**
is currently a Ph.D. candidate in the Department of Materials Science and Metallurgical Engineering, Kyungpook National University, Daegu, Korea, and is a member of the Advanced Mobility Components Group at the Korea Institute of Industrial Technology (KITECH). Her research interests include materials science.
E-mail: soobin35@kitech.re.kr

**Seong Uk Kwon**
is the CEO of Dae Sung Forge and received his B.S. degree from Daegu Catholic University, Korea. His research interests include plastic deformation and forging processes.
E-mail: daesungforge@naver.com

**Dae Cheol Ko**
is a Professor in the Department of Nanomechatronics Engineering at Pusan National University, Busan, Korea. His research fields include sheet metal forming, hot stamping, and green forming technology.
E-mail: dcko@pusan.ac.kr

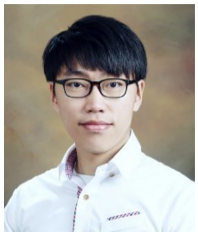

**Jin Seok Jang**
is a principal researcher at the Mobility Components Group of the Korea Institute of Industrial Technology. His research focuses on machinery system equipment diagnosis, vibration analysis, automation and monitoring of manufacturing processes, and machine vision.
E-mail: jsjang@kitech.re.kr